

# *Haemophilus ducreyi* Associates with Phagocytes, Collagen, and Fibrin and Remains Extracellular throughout Infection of Human Volunteers

MARGARET E. BAUER,<sup>1\*</sup> MICHAEL P. GOHEEN,<sup>2</sup> CARISA A. TOWNSEND,<sup>1</sup>  
AND STANLEY M. SPINOLA<sup>1,2,3</sup>

Departments of Medicine,<sup>1</sup> Pathology and Laboratory Medicine,<sup>2</sup> and Microbiology and Immunology,<sup>3</sup>  
Indiana University School of Medicine, Indianapolis, Indiana 46202

Received 6 November 2000/Returned for modification 3 January 2001/Accepted 11 January 2001

**In a previous study, *Haemophilus ducreyi* was found in the pustule and dermis of samples obtained at the clinical end point in the human model of infection. To understand the kinetics of localization, we examined infected sites at 0, 24, and 48 h after inoculation and at the clinical end point. Immediately after inoculation, bacteria were found predominantly in the dermis but also in the epidermis. Few bacteria were detectable at 24 h; however, by 48 h, bacteria were readily seen in the pustule and dermis. *H. ducreyi* was associated with polymorphonuclear leukocytes and macrophages in the pustule and at its base, but was not associated with T cells, Langerhans' cells, or fibroblasts. *H. ducreyi* colocalized with collagen and fibrin but not laminin or fibronectin. Association with phagocytes, collagen, and fibrin was seen as early as 48 h and persisted at the pustular stage of disease. Optical sectioning by confocal microscopy and transmission electron microscopy both failed to demonstrate intracellular *H. ducreyi*. These data identify collagen and fibrin as potentially important targets of adherence in vivo and strongly suggest that *H. ducreyi* remains extracellular throughout infection and survives by resisting phagocytic killing in vivo.**

*Haemophilus ducreyi* is the causative agent of chancroid, a sexually transmitted genital ulcer disease that facilitates the transmission of the human immunodeficiency virus (HIV). *H. ducreyi* enters the host through microabrasions that occur during intercourse and primarily remains localized in the skin. To study the pathogenesis of chancroid, we developed a human model of *H. ducreyi* infection in which volunteers are inoculated on the upper arm with *H. ducreyi* and observed until a painful pustule forms or disease resolves (4, 25, 26). The clinical course and the histopathology of experimental infection resemble naturally occurring disease (4, 20).

We recently reported methods to immunodetect *H. ducreyi* in pustules from experimentally infected volunteers (6). *H. ducreyi* was identified in these lesions with polyclonal anti-*H. ducreyi* antiserum, whose specificity was established by simultaneously staining sections with the polyclonal antiserum and a panel of monoclonal antibodies (MAbs) recognizing *H. ducreyi* surface antigens. In this study, we found that *H. ducreyi* is concentrated at the base of the pustule and is more sparsely distributed throughout the pustule and in the subpustular dermis. *H. ducreyi* did not associate with keratinocytes or fibroblasts. Within the pustule, *H. ducreyi* appears to associate with polymorphonuclear leukocytes (PMNs). These findings were limited to the pustular stage of disease, and we did not examine whether *H. ducreyi* interacted with other cells or structures in the skin.

In addition to components found in normal skin, pustules contain T cells, PMNs, and macrophages (20). In vitro, *H. du-*

*creyi* adheres to and invades keratinocytes and fibroblasts as well as epithelial cell lines (11, 15, 18, 19, 23, 30, 31), although invasion of fibroblasts is controversial (1, 19). *H. ducreyi* adheres to types I and III collagen, fibronectin, and laminin in vitro (5). Little is known about the interactions of *H. ducreyi* with these structures or cell types in vivo other than the organism's general location at the pustular stage of disease.

In the present study, we examined the association of *H. ducreyi* with PMNs, macrophages, T cells, fibroblasts, and Langerhans' cells at both the papular and pustular stages of disease. We also examined the association of the bacteria with dermal tissue components and whether *H. ducreyi* invades cells in vivo throughout experimental infection.

## MATERIALS AND METHODS

**Human subjects.** Volunteers included 21 healthy adults (mean age  $\pm$  standard deviation,  $35 \pm 10$  years; 13 women, 8 men) who participated in parent-mutant trials (3, 7, 9, 28, 32; R. S. Young, C. K. Ward, K. R. Fortney, B. P. Katz, A. F. Hood, E. J. Hansen, and S. M. Spinola, unpublished data) or who were infected or donated tissue specifically for this study (see Tables 1 and 2). Informed consent was obtained from the subjects for participation and for HIV serology in accordance with the human experimentation guidelines of the U.S. Department of Health and Human Services and the Institutional Review Board of Indiana University-Purdue University at Indianapolis. Enrollment procedures, exclusion criteria, inoculation protocols, and calculations of estimated delivered doses (EDD) have been described in detail elsewhere (25, 26).

**Tissue specimens.** Tissue specimens from infected sites were obtained by biopsy from 20 of the volunteers. Thirteen subjects were biopsied at the clinical end point, which is defined as development of a painful pustule, resolution of disease at all sites, or 14 days of infection. Two volunteers were inoculated at two sites each with 35000HP and biopsied immediately after inoculation (Table 1). Four volunteers were inoculated at three sites each with 35000HP and assigned to biopsy at 24 h or on the first day of pustule formation (Table 1). An additional volunteer was inoculated but only developed transient infection and was not biopsied. One volunteer donated uninfected tissue. All inoculated volunteers were treated with oral ciprofloxacin as described elsewhere (4).

Specimens were fixed in 4% paraformaldehyde and processed for microscopy

\* Corresponding author. Mailing address: Indiana University School of Medicine, Emerson Hall 435, 545 Barnhill Dr., Indianapolis, IN 46202. Phone: (317) 274-8143. Fax: (317) 274-1587. E-mail: mebauer@iupui.edu.

TABLE 1. Sources of tissue samples analyzed by confocal microscopy

Subject no.	Site <sup>a</sup>	Inoculum (CFU) <sup>b</sup>	Day of biopsy	Clinical outcome	<i>H. ducreyi</i> detected	Reference or source
102	P	53	8	Pustule	+	3
110	P	60	14	Pustule	+	3
111	P	120	7	Pustule	+	28
121	P	40	6	Pustule	+	32
121	M	32	6	Pustule	+	32
126	P	40	8	Pustule	+	32
126	M	32	8	Pustule	+	32
127	P	50	9	Pustule	+	32
128	P	50	8	Pustule	+	32
143	A/P	680	0	NA <sup>c</sup>	+	This study
143	B/P	680	0	NA	+	This study
146	A/P	570	0	NA	+	This study
146	B/P	57	0	NA	+	This study
138	A/P	41	1	Macule	-	This study
138	B/P	41	1	Papule	+	This study
167	A/P	64	1	Papule	-	This study
167	B/P	64	1	Papule	-	This study
149	A/P	64	2	Pustule	+	This study
149	B/P	64	2	Papule	+	This study
152	A/P	44	2	Papule	+	This study

<sup>a</sup> P, sites inoculated with *H. ducreyi* 35000 or 35000HP; M, sites inoculated with an isogenic mutant, A and B indicate different sites from the same subject.

<sup>b</sup> Estimated delivered dose.

<sup>c</sup> NA, not applicable.

as described previously (6), except that specimens were fixed for 3 h. Samples obtained for this study were initially examined for the presence of bacteria by staining every 10th section of each specimen with polyclonal antiserum raised against *H. ducreyi*, as described previously (6) (Table 1). To confirm that the structures recognized by the polyclonal antiserum were *H. ducreyi*, the specimens were simultaneously stained with the polyclonal serum and MAbs that recognize *H. ducreyi* antigens, as described (6).

**Primary Abs and stains.** *H. ducreyi* was detected with rabbit polyclonal antiserum raised against whole *H. ducreyi* cells (6, 13) and with murine MAb 5C9 or BB11, which recognize *H. ducreyi* lipoprotein (Hlp) (14) and the GroEL homolog heat shock protein (Hsp) (10), respectively.

Murine MAbs raised against human antigens included anti-CD1a MAb O10 (Beckman Coulter, Inc., Fullerton, Calif.) for Langerhans' cells, anti-CD3 MAb UCHT1 (Dako Corporation, Carpinteria, Calif.) for T cells, anti-CD45 MAb H130 for leukocytes (Pharmingen International, San Diego, Calif.), anti-CD68 MAb PG-M1 (Dako Corporation) for macrophages, antifibronectin MAb 568 (Novocastra Laboratories, Ltd., Burlingame, Calif.), and antilaminin MAb 4C7 (Dako Corporation). Rabbit polyclonal anti-human type I collagen antiserum was purchased from Novocastra Labs. Rabbit polyclonal anti-human fibrinogen was purchased from Dako Corp. Anti-multicytokeratin MAbs AE1 and AE3, antineutrophil elastase MAb NP57, antivimentin MAb VIM 3B4, and tetramethyl rhodamine isothiocyanate (TRITC)-labeled *Lens culinaris* agglutinin (LCA), used to stain eukaryotic cell membranes, were described previously (6).

**Secondary Abs.** Secondary Abs were purchased from Jackson Immuno-Research Laboratories (West Grove, Penn.) and have been described previously (6). These included goat anti-rabbit immunoglobulin G (IgG) and goat anti-mouse IgG which were affinity purified and conjugated with fluorescein isothiocyanate (FITC) or indodicarbocyanine (Cy5). Normal goat serum was also obtained from Jackson ImmunoResearch Laboratories.

Preliminary experiments showed that the secondary Abs cross-reacted with human leukocytes in the tissues. Thus, for sections stained with MAbs recognizing leukocyte antigens, the secondary Abs were absorbed with human leukocytes prior to use. To obtain leukocytes, whole blood was donated by a healthy adult volunteer after informed consent was obtained. Two volumes of 0.2% NaCl were added to hypotonically lyse erythrocytes, followed by 2 volumes of 1.6% NaCl. Cells were collected by centrifugation, and the process was repeated three to five times until no erythrocytes remained. Leukocytes were fixed by rocking for 15 min at room temperature in 4% paraformaldehyde in phosphate-buffered saline (PBS) (5) and washed three times in PBS.

Secondary Abs were diluted to a working concentration in PBS and subjected to two rounds of incubation with 10<sup>7</sup> paraformaldehyde-fixed leukocytes by rocking for 45 min at room temperature in the dark. Cells were removed by centrifugation before the Abs were used in staining.

**Immunofluorescence staining.** Tissue sections were stained as previously described (2, 6). Briefly, sections were permeabilized with Triton X-100, blocked with normal goat serum, stained with primary Ab, blocked again with normal goat serum, and incubated with fluorescently labeled secondary Ab. Sections stained with the anti-CD68 MAb were incubated in Retrieve-All antigen unmasking solution (Signet Pathology Systems, Inc., Dedham, Mass.) for 10 min at 92°C, followed by 10 min at room temperature, and washed three times in PBS prior to the permeabilization step. When used, TRITC-LCA was added simultaneously with the secondary Ab. Samples were mounted as described (6).

Negative controls were described previously (6) and included omitting each primary Ab, omitting each secondary Ab, and staining sections of uninfected upper arm skin. There was some background of tissue autofluorescence in the FITC channel; otherwise, no positive signals were observed in the negative controls.

**Confocal microscopy.** Stained sections were examined on a Bio-Rad MRC 1024 confocal laser scanning microscope. Samples examined for intracellular bacteria were optically sectioned in 0.2- $\mu$ m steps. Images were collected separately for FITC, TRITC, and Cy5 signals, and the images were colorized and combined using MetaMorph (Universal Imaging Corp., West Chester, Penn.) or Adobe Photoshop (Adobe Systems, Inc., San Jose, Calif.) software.

**TEM.** Specimens for transmission electron microscopy (TEM) were processed as described elsewhere (12). Briefly, specimens were fixed in 4% paraformaldehyde, embedded in LR White resin, sectioned, and stained with uranyl acetate and lead citrate. For immunogold labeling, sections were stained with rabbit polyclonal antiserum raised against whole *H. ducreyi* cells, followed by goat anti-rabbit IgG labeled with 15-nm gold particles.

## RESULTS

***H. ducreyi* delivered to epidermis and dermis during inoculation.** In the human model, bacteria are delivered into the skin via puncture wounds made by the tines of an allergy testing device (25, 26). To examine where *H. ducreyi* is placed in the skin, we inoculated two volunteers with 35000HP at two sites that were biopsied immediately after inoculation. One site was inoculated with an EDD of 50 CFU, and three sites were inoculated with an EDD of 500 CFU (Table 1). Specimens from these sites were processed as described above, and sections were doubly stained for *H. ducreyi* with polyclonal antiserum and the anti-*H. ducreyi* MAb 5C9 or BB11. A few sections from each specimen contained puncture wounds from the inoculation device. *H. ducreyi* was occasionally found along these puncture wounds (Fig. 1A). Although most of the bacteria were in the dermis, some *H. ducreyi* were found with keratinocytes in the epidermis (Fig. 1B). We also saw *H. ducreyi* along the epidermal surface of some sections (data not shown). These data show that *H. ducreyi* was delivered principally to the dermis but also to the epidermis in the human model.

**Kinetics of localization of *H. ducreyi*.** At the clinical end point, *H. ducreyi* bacteria are found in the pustule with PMNs, primarily clustered at the pustule base, and are also seen in the dermis (6). The organism does not colocalize with keratinocytes or fibroblasts at the pustular stage of disease (6). To examine the kinetics of localization, volunteers were infected with 35000HP and assigned to biopsy either at 24 h or on the first day of pustule formation. Specimens harvested included an erythematous macule, small papules from 24 h of infection, larger papules from 48 h, and newly formed pustules (Table 1). These samples, along with uninfected tissue and specimens harvested on day 0, were used to localize *H. ducreyi* with respect to PMNs, keratinocytes, and fibroblasts.

Small pockets of PMNs and fibroblasts were scattered in the dermis of uninfected tissue and tissue harvested on day 0 (Fig. 2A and data not shown). By 24 h, PMNs had infiltrated the

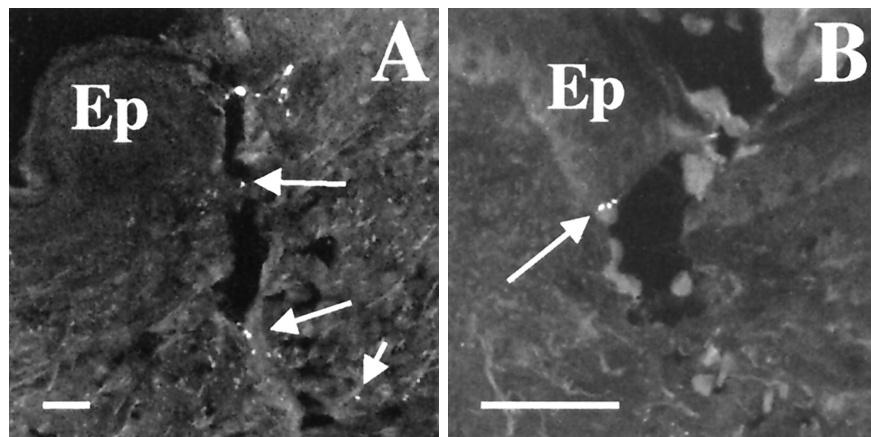


FIG. 1. Deposition of *H. ducreyi* in skin. Sections from tissue biopsied immediately postinoculation were stained with polyclonal anti-*H. ducreyi* antiserum and MAb BB11. (A) Puncture wound made by inoculation device. Arrows indicate bacteria along puncture wound. (B) Bacteria (arrow) at the epidermis with keratinocytes. Ep, epidermis. Bars, 50  $\mu$ m.

epidermis, forming small micropustules, and had collected in the dermis (Fig. 2B through D). Keratinocytes surrounding these micropustules were swollen, but the epidermis was intact (data not shown). More fibroblasts were evident at 24 h than in uninfected tissue (data not shown). *H. ducreyi* was found in only one section of one sample at 24 h (Table 1); therefore, we cannot make statements about bacterial localization at this time point.

At 48 h, the PMN infiltrate was more extensive, and samples had both intraepidermal micropustules and larger pustules

that merged with the dermal infiltrate (Fig. 2E and F). The 48-h specimens also contained greater numbers of fibroblasts, and keratinocyte swelling was still evident. In addition, the basilar epidermis was eroded by some pustules. Overall, little morphologic difference was observed at the microscopic level between samples clinically scored as papules and those scored as pustules (Fig. 2E and F). All specimens at 48 h contained *H. ducreyi* (Table 1), primarily at the base of pustules and in the subpustular dermis (Fig. 3A and B). A few bacteria were seen within the pustules associated with PMNs (data not shown).

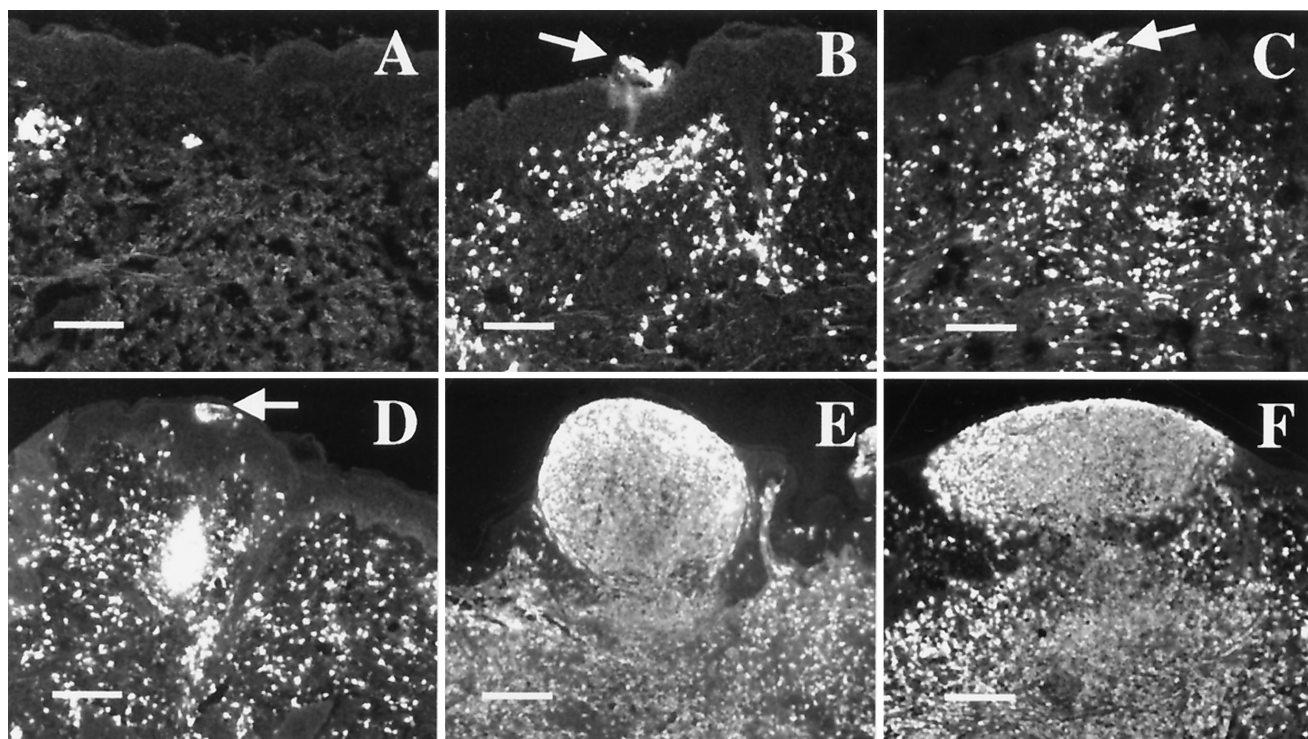


FIG. 2. Kinetics of lesion formation in the human model. Sections were stained with anti-PMN elastase. Panels represent tissue harvested immediately after inoculation (A), an erythematous macule at 24 h (B), papules at 24 h (C and D), a papule at 48 h (E), and a pustule at 48 h (F). Arrows indicate intraepidermal micropustules in 24-h samples. Bars, 150  $\mu$ m.

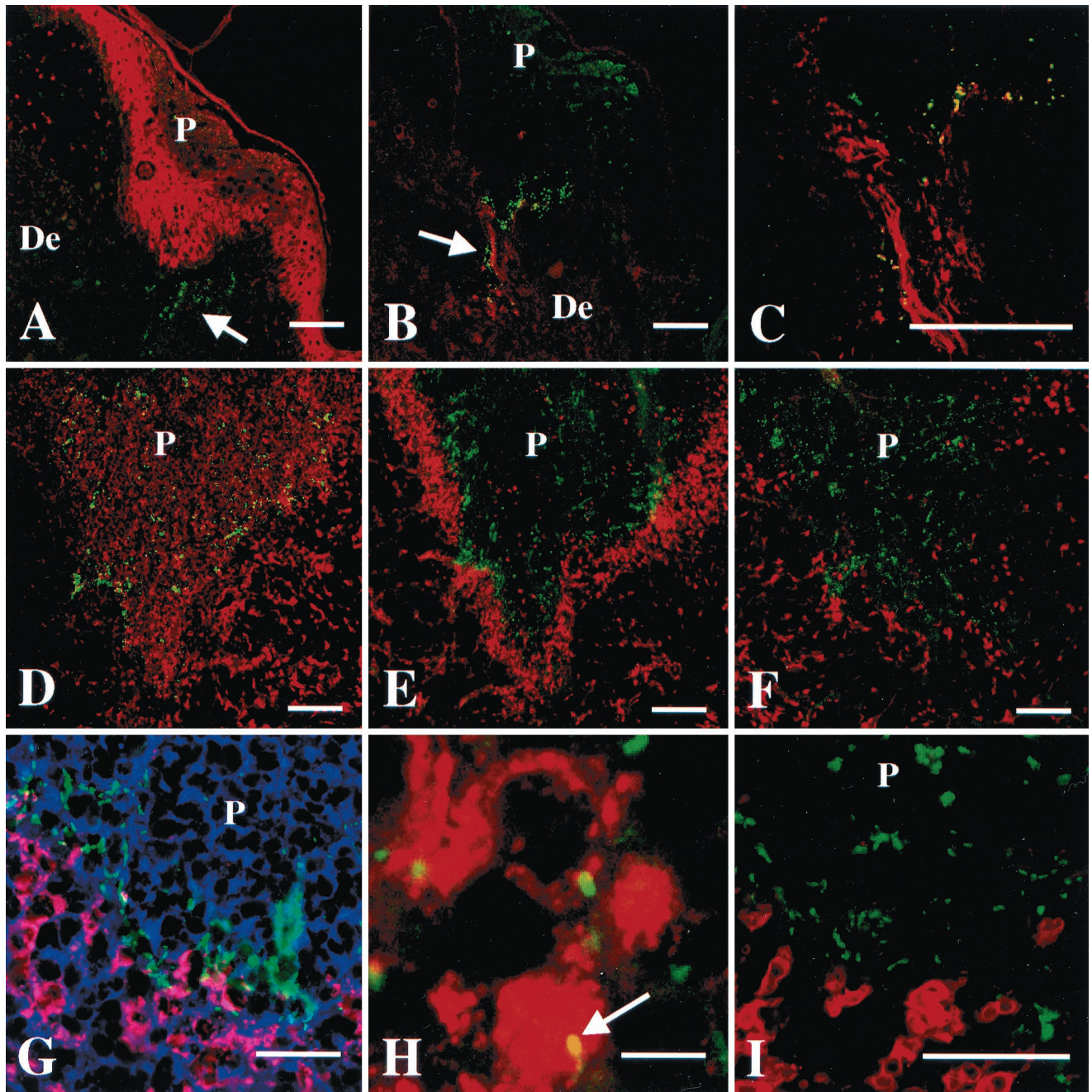


FIG. 3. Localization of *H. ducreyi* in tissues from papular and pustular stages of disease. P, pustule or micropustule. De, dermis. Scale bars represent 100  $\mu\text{m}$  in panels A through F, 50  $\mu\text{m}$  in panels G and I, and 5  $\mu\text{m}$  in panel H. (A) Papule at 48 h doubly stained with polyclonal anti-*H. ducreyi* antiserum (green) and anticytokeratin MAbs (red). Arrow indicates bacteria (green) in dermis below micropustule. (B) A 48-h papule doubly stained with polyclonal anti-type I collagen (red) and the anti-*H. ducreyi* MAb BB11 (green). Arrow indicates bacteria colocalizing with collagen (yellow). (C) Section stained as in panel B showing colocalization (yellow) of *H. ducreyi* and collagen. (D through F) Low-power view of consecutive sections from one pustule stained with polyclonal anti-*H. ducreyi* antiserum (green) and MAB recognizing PMN elastase (D), CD68 (E), or CD3 (F) (red). (G) Higher-power view of the base of a pustule. Section was stained with polyclonal anti-*H. ducreyi* antiserum (green), anti-CD68 (red), and the lectin LCA, which stains plasma membranes (blue). Colocalization of anti-CD68 (red) and LCA (blue) on the macrophage cell surface is represented in pink. Note the bacteria between the macrophages and the PMNs of the pustule. (H) High-power view of section stained with polyclonal anti-*H. ducreyi* antiserum (green) and anti-CD68 (red). Arrow indicates bacteria colocalizing with a macrophage (yellow). (I) Base of a pustule stained with polyclonal anti-*H. ducreyi* antiserum (green) and anti-CD3 (red). Note that the bacteria do not colocalize with the T cells.

*H. ducreyi* was found near keratinocytes at the pustule base but did not colocalize with them (Fig. 3A). Similarly, bacteria in the dermis were near fibroblasts, but no colocalization was observed (data not shown). Thus, *H. ducreyi* was found in the

dermis and pustule within 48 h of inoculation. Because no gross differences were observed between samples obtained at 48 h and at the clinical end point, no other time points were examined.

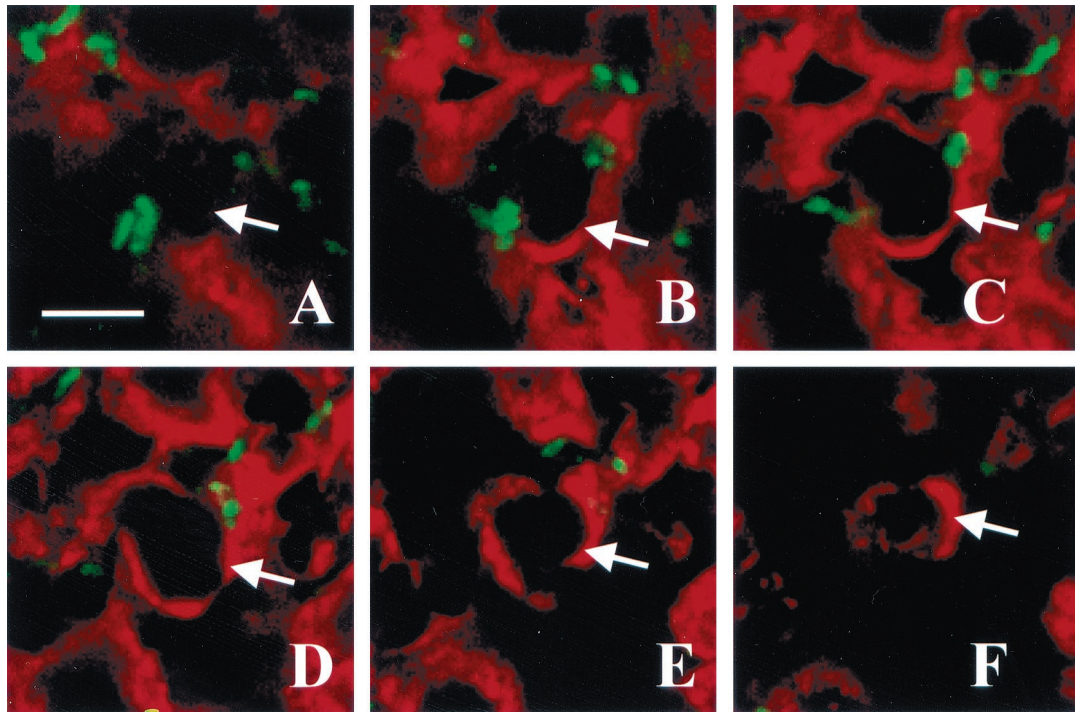


FIG. 4. Optical sectioning through a pustule. Panels A through F represent, in order, images taken in 1- $\mu$ m steps through a section stained with polyclonal anti-*H. ducreyi* antiserum (green) and anti-PMN elastase MAb (red). The arrow in each panel points to one edge of the PMN. Note the bacteria on the outside but not within the PMN. Bar, 5  $\mu$ m.

***H. ducreyi* associated with phagocytes in vivo.** Macrophages and PMNs are both recruited to sites of infection in the human model (20, 25, 26), and *H. ducreyi* is found with PMNs in vivo (6). To examine the interaction of *H. ducreyi* with macrophages, tissue sections were simultaneously stained for the bacteria and CD68. For comparison, consecutive tissue sections were doubly stained for *H. ducreyi* and PMNs. Macrophages had begun to infiltrate the dermis below micropustules by 24 h, and many macrophages were present throughout the upper dermis at 48 h. Macrophages were also occasionally seen in the pustules and micropustules (data not shown). *H. ducreyi* colocalized with macrophages in the dermis at 48 h (data not shown). At the clinical end point, most of the macrophages had coalesced into a band at the pustule base where the bacteria were most numerous (Fig. 3D and E). *H. ducreyi* was frequently associated with PMNs in the pustule. At the pustule base, *H. ducreyi* colocalized more commonly with PMNs (Fig. 3G), but the bacteria were also associated with macrophages (Fig. 3H). Thus, *H. ducreyi* associated with both these professional phagocytes in vivo.

***H. ducreyi* did not associate with Langerhans' cells.** Langerhans' cells are resident skin cells observed in specimens at the clinical end point (20, 25). To examine the interaction of *H. ducreyi* with Langerhans' cells, sections were doubly stained with polyclonal anti-*H. ducreyi* antiserum and an anti-CD1a MAb. In all specimens examined, including uninfected skin, Langerhans' cells resided in the epidermis and stained heavily in glands and hair follicles (data not shown). Very few CD1a<sup>+</sup> cells were found outside these areas, and CD1a<sup>+</sup> cells were not found in the pustule. *H. ducreyi* did not colocalize with the CD1a<sup>+</sup> cells (data not shown).

***H. ducreyi* did not associate with T cells.** T cells account for approximately 70% of the perivascular mononuclear cell infiltrate in lesions at the pustular stage of disease (20). To localize *H. ducreyi* with respect to T cells, tissue sections were doubly stained for *H. ducreyi* and CD3. Very few T cells were present in uninfected tissue, but small clusters of T cells were found at 24 and 48 h (data not shown). At the clinical end point, T cells were sparsely distributed throughout the upper dermis near the pustule (Fig. 3F). Dense pockets of T cells resided in the deep dermis (data not shown). In the subpustular dermis, *H. ducreyi* was occasionally found near T cells, but did not colocalize with them (Fig. 3I). The bacteria were rarely found in the deep dermis, and *H. ducreyi* did not colocalize with T cells in any specimen.

***H. ducreyi* did not invade cells in vivo.** *H. ducreyi* invades some eukaryotic cell types in vitro; however, it is not known whether the organism invades cells in vivo. In the present study, *H. ducreyi* associated with PMNs and macrophages but not with keratinocytes, T cells, or Langerhans' cells in vivo. To examine invasion by *H. ducreyi* in vivo, sections in which *H. ducreyi* associated with PMNs or macrophages in the *x/y* plane were subjected to optical sectioning along the *z* axis. We examined 2 to 17 independent fields in each of nine specimens. The optical sections were stacked and animated, which allowed the relative positions of the bacterial and eukaryotic cells to be examined in three dimensions. Figure 4 shows images taken at 1- $\mu$ m intervals through a section stained with polyclonal anti-*H. ducreyi* antiserum and an anti-PMN elastase MAb. In frozen sections, this MAb stains around the cell rather than in the cytoplasm. The bacteria were associated with the surface of cells but were not intracellular (Fig. 4). Similar results were

TABLE 2. Sources of tissue samples analyzed by TEM<sup>a</sup>

Subject no.	Site	Inoculum (CFU)	Day of biopsy	Clinical outcome	<i>H. ducreyi</i> detected	Reference or source
125	P	40	14	Pustule	—	32
128	P	50	8	Pustule	+	32
137	P	64	9	Pustule	—	32
147	P	89	7	Pustule	—	9
160	P	60	6	Pustule	—	7
164	P	93	7	Pustule	—	This study
172	P	50	7	Pustule	+	LspA1/2 trial <sup>b</sup>

<sup>a</sup> See Table 1, footnotes *a* and *b*.

<sup>b</sup> LspA, large supernatant protein (Young et al., unpublished data).

observed when sections were stained for the panleukocyte marker CD45 or for CD68 (data not shown). Overall, the bacteria were extracellular with respect to phagocytes.

In vivo, *H. ducreyi* was found in close proximity with fibroblasts but rarely colocalized with them (data not shown) (6). Since some investigators have reported that *H. ducreyi* invades this cell type in vitro (19), we examined specimens for invasion of fibroblasts in vivo. Sections were stained with an antivimentin MAb and polyclonal anti-*H. ducreyi* antiserum, and we optically sectioned areas that contained bacteria near fibroblasts. We found no evidence of bacteria colocalizing with or invading fibroblasts by this method (data not shown).

To search for intracellular *H. ducreyi* more closely, seven specimens from pustules harvested at the clinical end point were prepared for TEM (Table 2). Bacteria were found in only two specimens, most likely due to the relatively small number of *H. ducreyi* in the tissue (29). In one specimen, the bacteria were found only at the outer edge of the pustule and were surrounded by necrotic PMNs and eukaryotic cell debris (data not shown), which did not allow us to examine intracellularity. In the second specimen, bacteria were found at the base of the pustule among PMNs (Fig. 5A). Immunogold labeling with anti-*H. ducreyi* antiserum confirmed that the bacteria were

*H. ducreyi* (Fig. 5B). *H. ducreyi* were frequently surrounded by fibrin clots and were often seen adjacent to PMNs (Fig. 5A); however, no intracellular *H. ducreyi* were found.

***H. ducreyi* associated with fibrin in vivo.** TEM analysis suggested that *H. ducreyi* associated with fibrin in vivo. To examine this interaction by confocal microscopy, tissue sections were doubly stained with polyclonal antifibrinogen antiserum and the anti-*H. ducreyi* MAb BB11. Fibrin was present in the dermis at 24 and 48 h and formed a lattice throughout the pustules at 48 h and the clinical end point; little fibrin was seen in the micropustules at 24 h (Fig. 6F and data not shown). Numerous *H. ducreyi* colocalized with fibrin in the pustule, particularly at its base (Fig. 6F). At higher magnification, the fibrin appeared to surround the bacterial cells (Fig. 6G).

***H. ducreyi* associated with collagen in vivo.** *H. ducreyi* binds to type I and III collagen, fibronectin, and laminin in vitro (5). To localize the organism with respect to extracellular matrix (ECM) proteins in vivo, we simultaneously stained sections for *H. ducreyi* and MAbs recognizing type I collagen, fibronectin, or laminin.

The anticollagen MAb stained the dermis uniformly in uninfected tissue (data not shown). At 24 and 48 h, collagen stained most brightly in the dermis adjacent to the micropustules. At 48 h, the collagen signals were brightest where the bacteria were most numerous (Fig. 3B), and many bacteria colocalized with type I collagen in these areas (Fig. 3C). Similarly, at the clinical end point, the brightest collagen staining was at the pustule base where *H. ducreyi* was clustered (Fig. 6A). *H. ducreyi* frequently colocalized with collagen in this area (Fig. 6D) and often appeared to follow the contours of the collagen fibers (Fig. 6E).

In contrast to collagen, fibronectin stained most brightly in the subpustular dermis somewhat distal to the pustule base (Fig. 6B). Fibronectin and laminin outlined dermal capillaries (Fig. 6B and C). Laminin was present in the basement membrane, which was disrupted below pustules at 48 h and at the

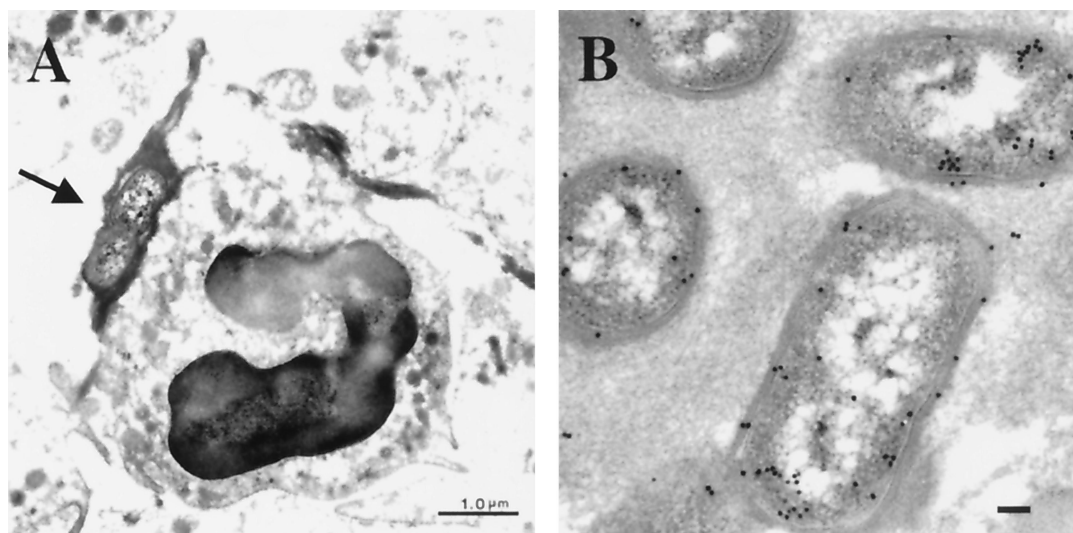


FIG. 5. Transmission electron micrographs of *H. ducreyi* in a pustule. (A) *H. ducreyi* at the base of the pustule surrounded by fibrin (arrow) and adjacent to a PMN. Bar, 1  $\mu$ m. (B) Immunogold labeling of *H. ducreyi* with polyclonal anti-*H. ducreyi* antiserum and gold-conjugated secondary Ab. Bar, 0.1  $\mu$ m.

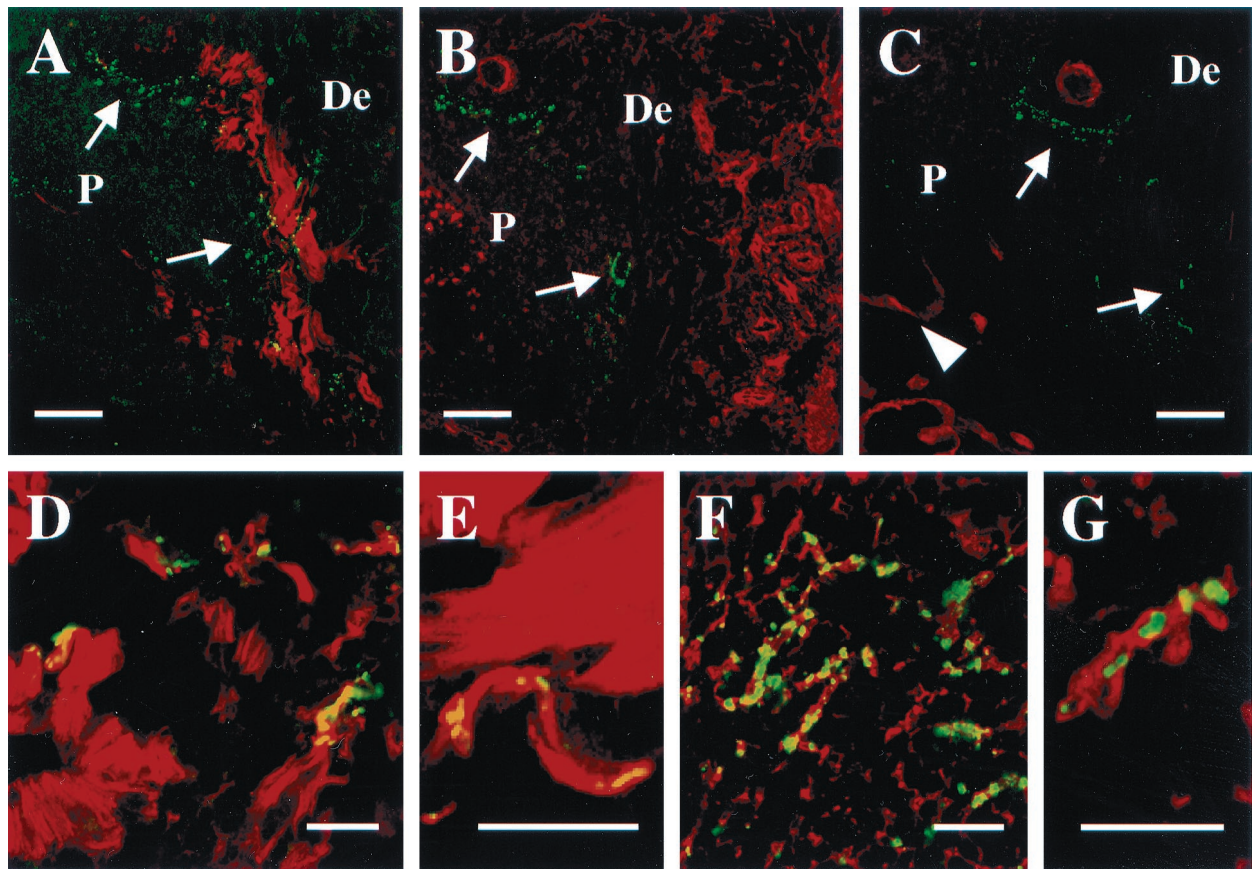


FIG. 6. *H. ducreyi* association with ECM proteins at the pustular stage. (A through C) Low-power images at the pustule base of consecutive tissue sections stained for *H. ducreyi* (green) and for collagen (A), fibronectin (B), or laminin (C) (red). Arrows indicate bacteria at the pustule base. Arrowhead in panel C indicates remains of the basement membrane. Bars, 100  $\mu\text{m}$ . (D) Section stained with polyclonal anti-type I collagen (red) and MAb BB11 (green). Note the colocalizing signals between collagen and *H. ducreyi* (yellow). Bar, 25  $\mu\text{m}$ . (E) Section stained as in panel D. Bar, 25  $\mu\text{m}$ . (F) Pustule within a section stained with polyclonal antifibrinogen (red) and the anti-*H. ducreyi* MAb BB11 (green). Note the colocalizing signals between the bacteria and the fibrin strands (yellow). Bar, 25  $\mu\text{m}$ . (G) Higher-power view of a section stained as in panel F, showing fibrin (red) surrounding *H. ducreyi* (green). Bar, 10  $\mu\text{m}$ .

clinical end point (Fig. 6C). *H. ducreyi* colocalized with fibronectin and laminin in only 1 of 12 specimens; otherwise, no association was observed between *H. ducreyi* and either fibronectin or laminin in vivo (data not shown). These data showed that *H. ducreyi* associated with type I collagen in vivo.

### DISCUSSION

In this study, we localized *H. ducreyi* in tissue samples from papular and pustular stages of disease in the human model of infection. At the clinical end point and as early as 48 h post-inoculation, *H. ducreyi* colocalized with PMNs, macrophages, collagen, and fibrin. The organism remained extracellular through the pustular stage of disease. Little to no colocalization was observed between *H. ducreyi* and other eukaryotic components, including keratinocytes, fibroblasts, Langerhans' cells, T cells, fibronectin, and laminin.

In this study, we included specimens from papules and pustules harvested at 24 and 48 h after inoculation. Consistent with an earlier study (20), the cellular infiltrate in these samples was similar to that of pustules from the clinical end point. The main difference was that the cellular infiltrate at 48 h had not yet coalesced into the organized pustule seen at the clinical

end point. The paucity of bacteria in samples harvested at 24 h precluded our ability to localize *H. ducreyi* that early. By 48 h, however, the bacteria were already present in the dermis and pustule, where they are found at the clinical end point. Furthermore, the associations of the bacteria with eukaryotic components seen at the clinical end point were under way by 48 h. Thus, the organism's location and its association with phagocytes, collagen, and fibrin began early in the disease process and remained unchanged through the pustular stage of disease.

The persistent association of *H. ducreyi* with PMNs and macrophages through the pustular stage suggests that the organism is able to resist killing and clearance by these professional phagocytes. Bacteria have evolved several mechanisms for countering the attacks of PMNs and macrophages. One such strategy is to survive or avoid phagocytosis. We detected no bacteria inside the phagocytes, suggesting that resistance to phagocytic killing is not due to intracellular survival after uptake. Rather, *H. ducreyi* may survive by either evading phagocytosis or escaping the phagocyte. Another strategy is to suppress or counteract the respiratory burst of PMNs, which is most effective on phagocytosed bacteria and those in close

apposition to the PMNs. *H. ducreyi* has been reported to both induce the PMN respiratory burst and resist its bactericidal effects in vitro (17). *H. ducreyi* produces a periplasmic copper- and zinc-dependent superoxide dismutase, which may protect the organism from the lethal effects of superoxide radicals produced by the respiratory burst (21, 22, 27).

Despite in vitro evidence that *H. ducreyi* can adhere to and invade keratinocytes (8, 11, 15), we found no evidence that *H. ducreyi* directly associates with keratinocytes at the papular or pustular stage of disease in vivo. The inoculation device punctures the skin to 1.9 mm, and the thickness of upper arm epidermis varies from 0.03 to 0.15 mm. Thus, we expected that most of the inoculum was delivered to the dermis. To test the possibility that this artificial route of inoculation bypassed the epidermis, we localized *H. ducreyi* immediately after inoculation. Although principally seen in the dermis, *H. ducreyi* was found in the epidermal layer, suggesting that the bacteria are available for interactions with keratinocytes in the human model. *H. ducreyi* may transiently attach to keratinocytes prior to 48 h; however, these data suggest that adherence to keratinocytes is not a major feature of experimental infection. The epidermal swelling around micropustules indicates that the keratinocytes are activated by 24 h and may play an important role in the host response to *H. ducreyi* by secreting cytokines such as interleukin-6 (IL-6) and IL-8 as has been shown in vitro (15, 33).

Although the ability of *H. ducreyi* to invade fibroblasts has been disputed (1), a number of other studies have shown that *H. ducreyi* invades fibroblasts and epithelial cell lines in vitro (18, 19, 23, 30, 31). We found no evidence by confocal microscopy or TEM of *H. ducreyi* invading these cell types in vivo. In adherence and invasion assays,  $10^6$  to  $10^7$  bacteria are allowed to interact with  $10^5$  eukaryotic cells. In the human model, infection is achieved with 1 to 100 CFU. Thus, invasion may occur at "pharmacologic" doses of the organism relative to the "physiologic" doses in the model. Additionally, in vitro assays cannot take into account all the complexities of the host environment and immune response. We cannot exclude the possibility that *H. ducreyi* invades cells at the ulcerative stage of disease or transiently prior to 48 h; however, invasion is not a significant part of the organism's life cycle at the papular and pustular stages.

*H. ducreyi* colocalized with fibrin in pustules, as evidenced by TEM and confocal microscopy. During cutaneous wound healing, fibrinogen is either released from platelets or produced by fibroblasts and is cleaved to make fibrin, which serves as a scaffolding for PMNs infiltrating the wounded site (16, 24). The organism's interaction with fibrin may occur via a receptor-ligand interaction or may be a less specific consequence of fibrin deposition in the area.

Collagen is the major component of the dermis, and *H. ducreyi* binds to type I and III collagen in vitro (5). In the present study, we showed that *H. ducreyi* colocalized with type I collagen in vivo. This interaction was seen as early as 2 days postinoculation and persisted at the pustular stage of disease. *H. ducreyi* did not bind, however, to fibronectin or laminin, which the organism binds to in vitro (5). These data demonstrate that binding to collagen but not fibronectin or laminin is a biologically relevant phenotype. Type I collagen is the dominant collagen form in normal skin. During cutaneous wound heal-

ing, collagen bundles are degraded by matrix metalloproteases, and new collagen is produced by fibroblasts (16, 24). The first collagen type laid down is type III, which is gradually replaced by type I collagen. These collagen types may be important targets of adherence for *H. ducreyi*. The organism's adherence to collagen but not keratinocytes in vivo may explain the need to abrade the skin in order for infection to occur.

From these results, we propose the following model of *H. ducreyi* pathogenesis. *H. ducreyi* shed from an infected site enters the skin through microabrasions that expose a collagen-rich dermis, which the organism may use for initial adherence and colonization. Bacterial components such as lipooligosaccharide and lipoproteins stimulate the innate immune system to recruit phagocytes and promote T-cell homing. Simultaneously, the process of normal cutaneous wound healing begins. Both processes involve expression of cytokines and chemoattractants by resident cells, including keratinocytes and fibroblasts. PMNs and macrophages are recruited to clear infection and cell debris from the wound. Existing ECM is degraded to allow migration of infiltrating cells through the dermis, while activated fibroblasts produce new collagen and fibrin that serve as a matrix for the migrating cells. A fibrin clot filled with phagocytes forms at the epidermal level. In the absence of infection, keratinocytes would migrate to close the wound and the fibrin clot would be sloughed. However, *H. ducreyi* persist at the base of the wound, and this continued bacterial presence stalls the wound-healing process at the inflammatory phase. Thus, the chancroidal lesion could be seen to represent the failure of a wound to heal because infection could not be cleared.

In summary, we have shown that *H. ducreyi* associates with PMNs, macrophages, collagen, and fibrin in vivo and that the organism remains extracellular through the pustular stage of disease. Experiments to extend these observations to the ulcerative stage with naturally occurring chancroid are in progress. These findings identify collagen and fibrin as potentially important targets of adherence and demonstrate that evasion of phagocytic killing may be critical to the survival of the bacteria and to the pathogenesis of disease.

#### ACKNOWLEDGMENTS

We thank Clifton Bong, Kate Fortney, Royden Young, and Beth Zwickl for help with the clinical trials, Exing Wang for assistance with the confocal microscope, Carrie Phillips for use of the cryostat, and Cathy Ison for providing MAb BB11. We thank Byron Batteiger, Antoinette Hood, and Tricia Humphreys for helpful review of the manuscript.

This work was supported by Public Health Service grants AI27863 and AI31494 from the National Institute of Allergy and Infectious Diseases (NIAID). M.E.B. was supported by Public Health Service grant AI09971 from the NIAID. The clinical samples used in this study were obtained from clinical trials supported by the Sexually Transmitted Diseases Clinical Trials Unit, through contract NO1-AI75329 from the NIAID, and by Public Health Service grants MO1RR00750, AI40263, AI38444, and AI32011 from the NIAID.

#### REFERENCES

- Alfa, M. J., P. Degagne, and T. Hollyer. 1993. *Haemophilus ducreyi* adheres to but does not invade cultured human foreskin cells. *Infect. Immun.* **61**: 1735-1742.
- Al-Tawfiq, J. A., M. E. Bauer, K. R. Fortney, B. P. Katz, A. F. Hood, M. Ketterer, M. A. Apicella, and S. M. Spinola. 2000. A pilus-deficient mutant of *Haemophilus ducreyi* is virulent in the human model of experimental infection. *J. Infect. Dis.* **181**:1176-1179.



3. Al-Tawfiq, J. A., K. R. Fortney, B. P. Katz, C. Elkins, and S. M. Spinola. 2000. An isogenic hemoglobin receptor-deficient mutant of *Haemophilus ducreyi* is attenuated in the human model of experimental infection. *J. Infect. Dis.* **181**:1049–1054.
4. Al-Tawfiq, J. A., A. C. Thornton, B. P. Katz, K. R. Fortney, K. D. Todd, A. F. Hood, and S. M. Spinola. 1998. Standardization of the experimental model of *Haemophilus ducreyi* infection in human subjects. *J. Infect. Dis.* **178**:1684–1687.
5. Bauer, M. E., and S. M. Spinola. 1999. Binding of *Haemophilus ducreyi* to extracellular matrix proteins. *Infect. Immun.* **67**:2649–2653.
6. Bauer, M. E., and S. M. Spinola. 2000. Localization of *Haemophilus ducreyi* at the pustular stage of disease in the human model of infection. *Infect. Immun.* **68**:2309–2314.
7. Bong, C. T. H., R. E. Throm, K. R. Fortney, B. P. Katz, A. F. Hood, C. Elkins, and S. M. Spinola. 2001. DsrA-deficient mutant of *Haemophilus ducreyi* is impaired in its ability to infect human volunteers. *Infect. Immun.* **69**:1488–1491.
8. Brentjens, R. J., S. M. Spinola, and A. A. Campagnari. 1994. *Haemophilus ducreyi* adheres to human keratinocytes. *Microb. Pathog.* **16**:243–247.
9. Fortney, K. R., R. S. Young, M. E. Bauer, B. P. Katz, A. F. Hood, R. S. Munson, Jr., and S. M. Spinola. 2000. Expression of peptidoglycan-associated lipoprotein is required for virulence in the human model of *Haemophilus ducreyi* infection. *Infect. Immun.* **68**:6441–6448.
10. Frisk, A., C. A. Ison, and T. Lagergard. 1998. GroEL heat shock protein of *Haemophilus ducreyi*: association with cell surface and capacity to bind to eukaryotic cells. *Infect. Immun.* **66**:1252–1257.
11. Gibson, B. W., A. A. Campagnari, W. Melaugh, N. J. Phillips, M. A. Apicella, S. Grass, J. Wang, K. L. Palmer, and R. S. Munson, Jr. 1997. Characterization of a transposon Tn916-generated mutant of *Haemophilus ducreyi* 35000 defective in lipooligosaccharide biosynthesis. *J. Bacteriol.* **179**:5062–5071.
12. Goheen, M. P., M. S. Bartlett, W. L. Current, M. M. Shaw, and J. W. Smith. 1994. Immunoelectron microscopy of *Pneumocystis carinii* exposed to a beta-1-3 glucan synthase inhibitor LY302146. *J. Eukaryot. Microbiol.* **41**:89S.
13. Hiltke, T. J., M. E. Bauer, J. Klesney-Tait, E. J. Hansen, R. S. Munson, Jr., and S. M. Spinola. 1999. Effect of normal and immune sera on *Haemophilus ducreyi* 35000HP and its isogenic MOMP and LOS mutants. *Microb. Pathog.* **26**:93–102.
14. Hiltke, T. J., A. A. Campagnari, and S. M. Spinola. 1996. Characterization of a novel lipoprotein expressed by *Haemophilus ducreyi*. *Infect. Immun.* **64**:5047–5052.
15. Hobbs, M. M., T. R. Paul, P. B. Wyrick, and T. H. Kawula. 1998. *Haemophilus ducreyi* infection causes basal keratinocyte cytotoxicity and elicits a unique cytokine induction pattern in an in vitro human skin model. *Infect. Immun.* **66**:2914–2921.
16. Kirsner, R. S., and W. H. Eaglstein. 1993. The wound healing process. *Dermatol. Clin.* **11**:629–640.
17. Lagergard, T., A. Frisk, M. Purven, and L. A. Nilsson. 1995. Serum bactericidal activity and phagocytosis in host defence against *Haemophilus ducreyi*. *Microb. Pathog.* **18**:37–51.
18. Lagergard, T., M. Purven, and A. Frisk. 1993. Evidence of *Haemophilus ducreyi* adherence to and cytotoxin destruction of human epithelial cells. *Microb. Pathog.* **14**:417–431.
19. Lammel, C. J., N. P. Dekker, J. Palefsky, and G. F. Brooks. 1993. In vitro model of *Haemophilus ducreyi* adherence to and entry into eukaryotic cells of genital origin. *J. Infect. Dis.* **167**:642–650.
20. Palmer, K. L., C. T. Schnizlein-Bick, A. Orazi, K. John, C.-Y. Chen, A. F. Hood, and S. M. Spinola. 1998. The immune response to *Haemophilus ducreyi* resembles a delayed-type hypersensitivity reaction throughout experimental infection of human subjects. *J. Infect. Dis.* **178**:1688–1697.
21. San Mateo, L. R., M. M. Hobbs, and T. H. Kawula. 1998. Periplasmic copper-zinc superoxide dismutase protects *Haemophilus ducreyi* exogenous superoxide. *Mol. Microbiol.* **27**:391–404.
22. San Mateo, L. R., K. L. Toffer, P. E. Orndorff, and T. H. Kawula. 1999. Neutropenia restores virulence to an attenuated Cu, Zn superoxide dismutase-deficient *Haemophilus ducreyi* strain in the swine model of chancroid. *Infect. Immun.* **67**:5345–5351.
23. Shah, L., H. A. Davies, and R. A. Wall. 1992. Association of *Haemophilus ducreyi* with cell-culture lines. *J. Med. Microbiol.* **37**:268–272.
24. Singer, A. J., and R. A. F. Clark. 1999. Cutaneous wound healing. *N. Engl. J. Med.* **341**:738–746.
25. Spinola, S. M., A. Orazi, J. N. Arno, K. Fortney, P. Kotylo, C.-Y. Chen, A. A. Campagnari, and A. F. Hood. 1996. *Haemophilus ducreyi* elicits a cutaneous infiltrate of CD4 cells during experimental human infection. *J. Infect. Dis.* **173**:394–402.
26. Spinola, S. M., L. M. Wild, M. A. Apicella, A. A. Gaspari, and A. A. Campagnari. 1994. Experimental human infection with *Haemophilus ducreyi*. *J. Infect. Dis.* **169**:1146–1150.
27. Stevens, M. K., D. J. Hassett, J. D. Radolf, and E. J. Hansen. 1996. Cloning and sequencing of the gene encoding the Cu, Zn-superoxide dismutase of *Haemophilus ducreyi*. *Gene* **183**:35–40.
28. Throm, R. E., J. A. Al-Tawfiq, K. R. Fortney, B. P. Katz, A. F. Hood, E. J. Hansen, and S. M. Spinola. 2000. Evaluation of an isogenic MOMP-deficient mutant in the human model of *Haemophilus ducreyi* infection. *Infect. Immun.* **68**:2602–2607.
29. Throm, R. E., and S. M. Spinola. 2001. Transcription of candidate virulence genes of *Haemophilus ducreyi* during infection of human volunteers. *Infect. Immun.* **69**:1483–1487.
30. Totten, P. A., J. C. Lara, D. V. Norn, and W. E. Stamm. 1994. *Haemophilus ducreyi* attaches to and invades human epithelial cells in vitro. *Infect. Immun.* **62**:5632–5640.
31. Wood, G. E., S. M. Dutro, and P. A. Totten. 1999. Target cell range of *Haemophilus ducreyi* hemolysin and its involvement in invasion of human epithelial cells. *Infect. Immun.* **67**:3740–3749.
32. Young, R. S., K. R. Fortney, V. Gelfanova, C. L. Phillips, B. P. Katz, A. F. Hood, J. L. Latimer, R. S. Munson, Jr., E. J. Hansen, and S. M. Spinola. 2001. Expression of cytolethal distending toxin and hemolysin are not required for pustule formation by *Haemophilus ducreyi* in human volunteers. *Infect. Immun.* **69**:1938–1942.
33. Zaretzky, F. R., and T. H. Kawula. 1999. Examination of early interactions between *Haemophilus ducreyi* and host cells by using cocultured HaCaT keratinocytes and foreskin fibroblasts. *Infect. Immun.* **67**:5352–5360.